

# Phase-sensitive evidence of pair-density-wave order in a cuprate

P. M. Lozano,<sup>1,2</sup> Tianhao Ren,<sup>1</sup> G. D. Gu,<sup>1</sup> A. M. Tsvelik,<sup>1</sup>  
J. M. Tranquada,<sup>1\*</sup> and Qiang Li<sup>1,2\*</sup>

<sup>1</sup>Condensed Matter Physics and Materials Science Division,  
Brookhaven National Laboratory, Upton, New York 11973-5000, USA

<sup>2</sup>Department of Physics and Astronomy, Stony Brook University,  
Stony Brook, New York 11794-3800, USA

\*To whom correspondence should be addressed;  
E-mail: jtran@bnl.gov (J.M.T.); liqiang@bnl.gov (Q.L.)

**Charge order is commonly believed to compete with superconducting order. An intertwined form of superconducting wave function, known as pair-density-wave (PDW) order, has been proposed; however, there has been no direct evidence, theoretical or experimental, forms the ground state of any cuprate superconductor. As a test case, we consider  $\text{La}_{2-x}\text{Ba}_x\text{CuO}_4$  with  $x = 1/8$ , where charge and spin stripe orders within the  $\text{CuO}_2$  planes compete with three-dimensional superconducting order. We report measurements of the superconducting critical current perpendicular to the planes in the presence of an in-plane magnetic field. The variation of the critical current with orientation of the field precisely confirms a theoretical prediction unique to the PDW model. This observation has direct implications for the pairing mechanism.**

In a superconductor, a collective state of paired electrons supports dissipationless transport, corresponding to current flow without resistance. For a solid with charge order, there is a static spatial modulation of the density of conduction electrons. While charge order has now been observed in most cuprate superconductors (1, 2), charge and superconducting orders are typically viewed as competitors (3–6). An extreme case occurs in  $\text{La}_{2-x}\text{Ba}_x\text{CuO}_4$  (LBCO) with  $x = 1/8$ , where the crystal structure at low temperature has anisotropic Cu-O bonds that stabilize charge and spin stripe orders (7, 8). Unusual two-dimensional (2D) superconductivity develops at the onset of spin-stripe order (9, 10).

Evidence for the 2D superconductivity is illustrated in Fig. 1a, where one can see that the in-plane resistivity, labelled  $\rho_b$ , in the absence of a magnetic field shows a substantial drop at  $\sim 40$  K, indicating the onset of phase-disordered superconductivity, with phase order developing below 20 K in the form of a Berezinskii-Kosterlitz-Thouless transition (9). Meanwhile, the resistivity along the  $c$  axis,  $\rho_c$  (measured perpendicular to the planes), remains large until the temperature drops below 10 K, demonstrating the 2D character of the superconducting fluctuations. Application of a strong in-plane magnetic field lowers these transition temperatures, but they remain finite.

It is extremely unusual to observe 2D superconductivity within equivalent layers of a bulk crystal because one would normally expect some type of effective Josephson coupling between neighboring layers that results in three-dimensional superconducting order. To explain the apparent frustration of the interlayer Josephson coupling (9, 11), PDW order was proposed (12–14). In this state, the pair wave function has extrema on the charge stripes, where the amplitude oscillates from positive to negative on neighboring charge stripes. The suggested PDW state corresponds to a situation where the superconducting pairs have finite momenta along the direction of the charge modulation. The frustration of the interlayer coupling comes from a 90° rotation of the PDW order between layers, following the pinning of the charge stripes

to the lattice anisotropy (15), as indicated in the upper inset of Fig. 1a.

While the PDW proposal is consistent with experiment, its relevance remains uncertain. The PDW is a strongly-correlated state that is difficult to reconcile with the conventional theory of superconductivity (16), which is based on a model of nearly-free, spatially-extended electron waves. On the other hand, evaluations of relevant theoretical models appropriate to hole-doped cuprates using advanced numerical techniques find that, while there is evidence for charge- and spin-stripe orders for a hole concentration of 1/8, the measure of superconducting coherence is strongly depressed and spatially uniform (17–19). Calculations show that the PDW state is close in energy to other solutions (20), but none have identified conditions where it is the ground state.

Fortunately, Yang (21) proposed an experimental test directly sensitive to the PDW state proposed for LBCO. He noted that the mismatch between the momenta of the Cooper pairs located in adjacent  $\text{CuO}_2$  planes can be reduced by application of an in-plane magnetic field (22); measurements on the closely-related compound  $\text{La}_{1.7}\text{Eu}_{0.2}\text{Sr}_{0.1}\text{CuO}_4$  have demonstrated that a strong in-plane field can reduce  $\rho_c$  (23). A phase-sensitive prediction is that the superconducting critical-current density along the  $c$  axis should be maximum when the field is at  $45^\circ$  to the Cu-O bonds. As we will show, our measurements are in agreement with this prediction. We consider this to be direct evidence for PDW order in our LBCO sample. Furthermore, we will argue that this state must be independent of any spatially-uniform superconductivity in the sample, which means that PDW order in conjunction with spin-stripe order competes with spatially-uniform superconductivity.

The anticipated anisotropy is already apparent in the resistive state that exists below 30 K, the onset of phase-disordered 2D superconductivity in the presence of a 14-T magnetic field applied parallel to the planes. The variation of  $\rho_c$  as a function of the field orientation with respect to the Cu-O bonds is shown in Fig. 1b. Here, the Cu-O bond directions are identified

as the  $a$  and  $b$  axes; these axes are equivalent, so the specific labelling is arbitrary. As one can see,  $\rho_c$  exhibits minima when the applied field is at  $45^\circ$  to the  $a$  and  $b$  axes, with the relative magnitude of the modulation growing as the temperature decreases.

The lack of perfect 4-fold symmetry is a consequence of the sample shape. The crystal for this measurement is longest along  $c$ , and it has unequal widths of the  $a$  and  $b$  faces (see Supplementary Material). This leads to anisotropy in the demagnetization factor (24), which means that the internal magnetic field is not precisely identical when the field is along  $a$  or  $b$ .

For comparison, we show the impact of field orientation on  $\rho_b$  in Fig. 1c. In this geometry, we have an anisotropy that is controlled by the orientation of the field relative to the measurement current, which is along  $b$ , resulting from the Lorentz force on magnetic vortices. The resistivity is a minimum when the current is parallel to the applied field, which means that we have a two-fold variation, and not the four-fold modulation of  $\rho_c$ .

To explore the critical-current density along the  $c$  axis, we have to cool to below 5 K. Figure 2a shows examples of voltage vs. current measurements for field along the  $a$  axis and temperatures from 4 K down to 1.9 K. Following standard procedure, we identify the critical current as the value at which the voltage crosses a threshold value indicated by the dashed line, which corresponds to an electric field along the  $c$  axis of  $1 \mu\text{V}/\text{cm}$ .

The variation of the  $c$ -axis critical-current density,  $J_c$ , with field angle is plotted in Fig. 2b. As one can see, it peaks periodically at odd multiples of  $45^\circ$ , thus confirming the theoretical prediction for the PDW model (21). Figure 2c shows that the effect is detectable with magnetic fields of smaller magnitude, as well. Of course, at fixed temperature there is a large change in  $J_c$  with field magnitude due to its effect on the superconductivity in the  $\text{CuO}_2$  planes, as one can see in Fig. 1a.

Now that we have established the main point, we can consider some finer issues. In particular, the decrease of  $\rho_c$  below  $\sim 25$  K is not what one would expect from an ideal system of

2D superconducting layers with a uniformly-frustrated interlayer Josephson coupling. The observed  $T$ -dependence of  $\rho_c$  exhibits a very fast drop resembling the behavior of one-dimensional (1D) superconducting nanowires in which phase slips result in finite resistivity (25). It suggests that in the temperature interval between 4 and  $\sim 25$  K we have the peculiar situation of two types of liquids of superconducting pairs: one type involving 2D PDW order, and the other type consisting of pairs located on effective nanowires traversing the sample along the  $c$  direction. It is important to note that the effective 1D superconducting fluctuations along  $c$  must be decoupled from the 2D PDW superconductivity. If they were coherent with one another, this would provide an interlayer coupling between the PDW order in the layers and the superconductivity would immediately become 3D. One likely origin of such a situation lies in charge inhomogeneities. As discussed in detail elsewhere (26), charge disorder is significant in cuprates, as demonstrated by local probes such as nuclear magnetic resonance (27). Hence, we can expect to have some patches in each plane with a local hole concentration  $\gtrsim 0.14$  that can support spatially-uniform superconductivity. Some of these patches will be able to couple along the  $c$  axis, causing  $\rho_c$  to drop. A subset of these may form effective 1D “trails” crossing the sample. Another contribution may come from crystallographic twin boundaries, where the local variation in symmetry (28) might allow finite patches of uniform superconductivity that could communicate along the  $c$  axis.

For  $c$ -axis transport at low temperature, we must once again take account of the superconducting layers. The effectiveness of the PDW order at frustrating the phase-coupling of neighboring layers is limited by the finite correlation lengths of the charge-stripe domains (8). At some point, we expect that the net interlayer coupling can result in 3D superconducting order. In particular, at temperatures of 4 K and below, there may be multiple contributions to the critical current measurement. The key point is that only the PDW contribution is sensitive to the orientation of the in-plane magnetic field.

There have been several previous reports of local PDW order by scanning tunneling microscopy. These include detecting PDW order in the vicinity of magnetic vortex cores through interference with uniform superconductivity (29), through local periodic modulations of the superconducting gap (30), and from Josephson tunneling into regions of periodically-modulated superfluid density (31). It is possible that local perturbations, such as a magnetic vortex core, may change the energy balance, stabilizing PDW locally even when the energetically-favored order in the bulk is spatially-uniform superconductivity. The present results are distinct, as they demonstrate that conditions in LBCO are such that PDW order is favored in the ground state. Another distinguishing feature is the presence of spin-stripe order.

We conclude that the PDW order in our sample is intertwined with spin-stripe order (10). Such local antiferromagnetic order is incompatible with spatially-uniform superconductivity, due to the strongly-correlated character of the magnetism, thus resulting in the indirect competition of the two forms of superconducting order. Within the PDW phase, the pairing correlations must develop within the charge stripes. The original proposal for pairing on charge stripes assumed that the spin stripes have a spin gap (32); the present case of ordered spin stripes requires that the spin gap be associated with charge stripes. A natural model for charged stripes with a spin gap is that of the hole-doped two-leg spin ladder (33, 34), which has been argued to be consistent with the spin excitations measured by neutron scattering (26). When the spin stripes can be disordered and gapped, essentially the same mechanism may explain the spatially-uniform superconductivity that is most common in the cuprates (35, 36). Hence, PDW order in LBCO may be the exception that proves the rule.

## References

1. R. Comin, A. Damascelli, *Annu. Rev. Condens. Matter Phys.* **7**, 369 (2016).

2. A. Frano, S. Blanco-Canosa, B. Keimer, R. J. Birgeneau, *J. Phys. Condens. Matter* **32**, 374005 (2020).
3. B. Keimer, S. A. Kivelson, M. R. Norman, S. Uchida, J. Zaanen, *Nature* **518**, 179 (2015).
4. M. Imada, *J. Phys. Soc. Jpn.* **90**, 111009 (2021).
5. J. Chang, *et al.*, *Nat. Phys.* **8**, 871 (2012).
6. Y. Caplan, G. Wachtel, D. Orgad, *Phys. Rev. B* **92**, 224504 (2015).
7. M. Fujita, H. Goka, K. Yamada, J. M. Tranquada, L. P. Regnault, *Phys. Rev. B* **70**, 104517 (2004).
8. M. Hücker, *et al.*, *Phys. Rev. B* **83**, 104506 (2011).
9. Q. Li, M. Hücker, G. D. Gu, A. M. Tsvelik, J. M. Tranquada, *Phys. Rev. Lett.* **99**, 067001 (2007).
10. E. Fradkin, S. A. Kivelson, J. M. Tranquada, *Rev. Mod. Phys.* **87**, 457 (2015).
11. S. Tajima, T. Noda, H. Eisaki, S. Uchida, *Phys. Rev. Lett.* **86**, 500 (2001).
12. A. Himeda, T. Kato, M. Ogata, *Phys. Rev. Lett.* **88**, 117001 (2002).
13. E. Berg, *et al.*, *Phys. Rev. Lett.* **99**, 127003 (2007).
14. D. F. Agterberg, *et al.*, *Annu. Rev. Condens. Matter Phys.* **11**, 231 (2020).
15. M. v Zimmerman, *et al.*, *Europhys. Lett.* **41**, 629 (1998).
16. J. Bardeen, L. N. Cooper, J. R. Schrieffer, *Phys. Rev.* **108**, 1175 (1957).
17. S. R. White, D. J. Scalapino, *Phys. Rev. B* **79**, 220504 (2009).

18. S. R. White, D. J. Scalapino, *Phys. Rev. B* **92**, 205112 (2015).
19. S. Jiang, D. J. Scalapino, S. R. White, Ground State Phase Diagram of the  $t$ - $t'$ - $J$  model (2021).
20. P. Corboz, T. M. Rice, M. Troyer, *Phys. Rev. Lett.* **113**, 046402 (2014).
21. K. Yang, *J. Supercond. Nov. Magn.* **26**, 2741 (2013).
22. K. Yang, D. F. Agterberg, *Phys. Rev. Lett.* **84**, 4970 (2000).
23. Z. Shi, P. G. Baity, J. Terzic, T. Sasagawa, D. Popović, *Nat. Commun.* **11**, 3323 (2020).
24. R. Prozorov, V. G. Kogan, *Phys. Rev. Applied* **10**, 014030 (2018).
25. A. Rogachev, A. Bezryadin, *Appl. Phys. Lett.* **83**, 512 (2003).
26. J. M. Tranquada, *Adv. Phys.* **69**, 437 (2020).
27. P. M. Singer, A. W. Hunt, T. Imai, *Phys. Rev. Lett.* **88**, 047602 (2002).
28. Y. Zhu, *et al.*, *Phys. Rev. Lett.* **73**, 3026 (1994).
29. S. D. Edkins, *et al.*, *Science* **364**, 976 (2019).
30. Z. Du, *et al.*, *Nature* **580**, 65 (2020).
31. M. H. Hamidian, *et al.*, *Nature* **532**, 343 (2016).
32. V. J. Emery, S. A. Kivelson, O. Zachar, *Phys. Rev. B* **56**, 6120 (1997).
33. E. Dagotto, T. M. Rice, *Science* **271**, 618 (1996).
34. A. M. Tsvelik, *Phys. Rev. B* **83**, 104405 (2011).

35. H.-C. Jiang, S. A. Kivelson, Stripe order enhanced superconductivity in the Hubbard model, arXiv:2105.07048 (2021).
36. Y. Li, *et al.*, *Phys. Rev. B* **98**, 224508 (2018).

**Acknowledgments:** We acknowledge helpful comments from E. H. Fradkin, S. A. Kivelson, V. Oganesyan, and K. Yang. **Funding:** This work was supported by the U.S. Department of Energy, Office of Basic Energy Sciences, Division of Materials Sciences and Engineering, under Contract No. DE-SC0012704. **Author Contributions:** Q.L. designed, and together with J.M.T., directed the study. G.D.G. grew the crystals. P.M.L. and Q.L. performed the transport measurements. All authors made contributions to analyzing the results and writing the manuscript. **Competing Interests:** The authors declare no competing financial interests.

**Data availability:** All data are available in the main text.

**Materials and Methods:** Single crystals of LBCO with  $x = 1/8$  studied here were grown in an infrared image furnace by the floating-zone technique. They are pieces from the same cylindrical crystal used previously to characterize two-dimensional fluctuating superconductivity (9). Single-crystal samples were cut and aligned into slabs, then fixed on a 0.5-mm-thick sapphire substrate. The imperfection in the sample alignment, estimated from X-ray diffraction, is less than 0.5 degree. For transport measurements, current contacts were made at the ends of the longest dimension of crystals (*e.g.*, a *c*-axis-oriented crystal with dimensions along axes  $c \times b \times a$  of  $3.50 \times 0.94 \times 0.20$  mm<sup>3</sup>) to ensure uniform current flow, while the voltage contacts were made on both the top and side of the crystals. We used a low-temperature contact annealing procedure (9) leading to low contact resistance ( $< 0.2 \Omega$ ) that allows us to measure the resistivity over seven orders of magnitude. The angular-resolved magnetoresistance (ARMR) was measured using the 4-point probe in-line method in a Quantum Design Physical Property Measurement System (PPMS) equipped with a 14-T superconducting magnet. The resistivity

measurements have been performed with the current applied along either the  $a(b)$ -direction or the  $c$ -direction using dc and ac transport options with a current range of  $50 \mu\text{A} - 1 \text{ mA}$ . Both dc and ac methods produced the same results. The data shown are from the ac transport measurements (17 Hz). For crystal alignment with magnetic field, horizontal and vertical sample rotators were used with the angular resolution  $\sim 0.1^\circ$ . Temperature dependent ARM data were taken from 1.8 to 300 K, at various fields up to 14 T. ARM data at fixed temperatures and magnetic fields were taken in-situ with a vertical sample rotator as a function of the in-plane magnetic field angles ( $\theta$ ) in a range of  $-15^\circ$  to  $360^\circ$ .

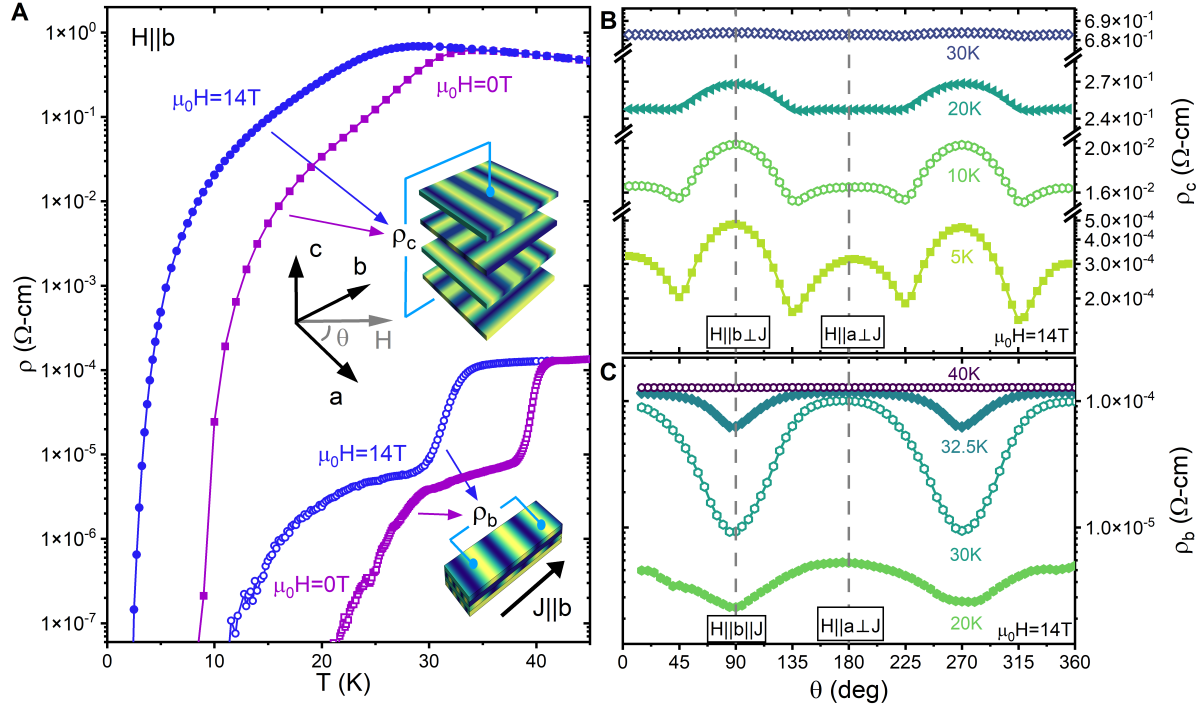
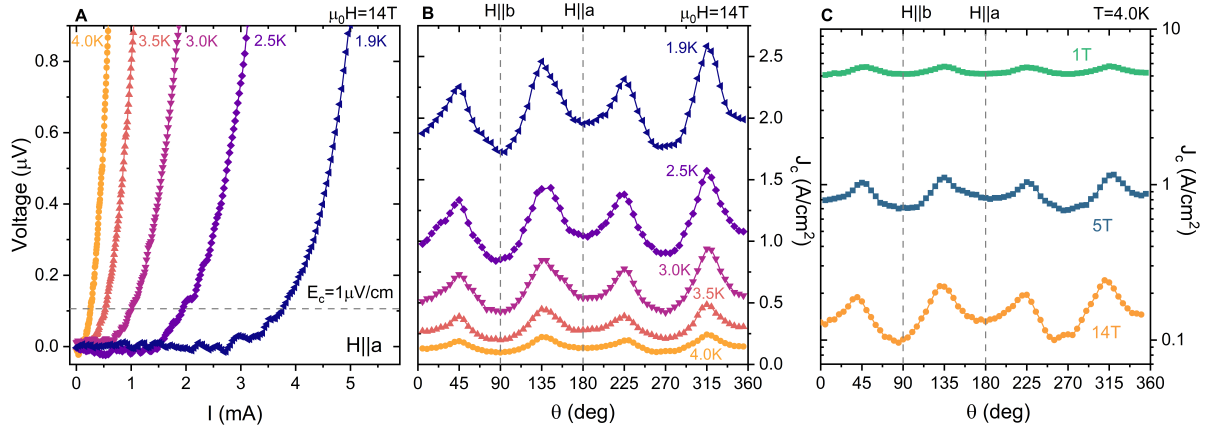


Figure 1: **Response of anisotropic resistivity to an in-plane magnetic field of 14 T.** **a**, Resistivity vs. temperature for  $\rho_b$  (open symbols) and  $\rho_c$  (filled symbols) in zero field (magenta circles) and full field applied along the  $b$  axis (blue squares), corresponding to field angle  $\theta = 90^\circ$  measured relative to the  $a$  axis. ( $a$  and  $b$  are equivalent, and correspond to Cu-O bond directions.) Upper inset indicates the proposed PDW order, with the superconducting wave function oscillating from positive (dark) to negative (light), and rotating by  $90^\circ$  between layers. Insets also indicate relative positions of voltage contacts. **b**, Variation of  $\rho_c$  with  $\theta$  at  $T = 5, 10, 20$ , and  $30$  K. **c**, Variation of  $\rho_b$  with  $\theta$  at  $T = 20, 30, 32.5$ , and  $40$  K.



**Figure 2: Behavior of the critical current density along the  $c$  axis with an in-plane magnetic field.** **a**, Examples of voltage vs. current applied along the  $c$  axis with the magnetic field of 14 T along the  $a$  axis ( $\theta = 0$ ) for several temperatures. Dashed line indicates the threshold criterion, corresponding to an electric field  $E_c = 1\text{\textmu V/cm}$ , used to determine the critical current. **b**, Variation of the critical current density along  $c$ ,  $J_c$ , with field angle  $\theta$  for several temperatures and a magnetic field of 14 T. Maxima are distinctly aligned with the directions at  $45^\circ$  to the Cu-O bond directions. **c**, Similar to **b**, but comparison of results for three values of the magnetic field (1, 5, and 14 T) at  $T = 4\text{ K}$ ; note that the scale for  $J_c$  is logarithmic.